condensed matter

MDPI

Article

Euclidean Q-Balls of Fluctuating SDW/CDW in the 'Nested' Hubbard Model of High-T_c Superconductors as the Origin of Pseudogap and Superconducting Behaviors

Sergei Mukhin

Theoretical Physics and Quantum Technologies Department, NUST "MISIS", Leninskiy Ave. 4, 119049 Moscow, Russia; si.muhin@misis.ru; Tel.: +7-495-955-0062

Abstract: The origin of the pseudogap and superconducting behaviors in high-T_c superconductors is proposed, based on the picture of Euclidean Q-balls formation that carry Cooper/local-pair condensates inside their volumes. Euclidean Q-balls that describe bubbles of collective spin-/charge density fluctuations (SDW/CDW) oscillating in Matsubara time are found as a new self-consistent solution of the Eliashberg equations in the 'nested' repulsive Hubbard model of high-T_c superconductors. The Q-balls arise due to global invariance of the effective theory under the phase rotation of the Fourier amplitudes of SDW/CDW fluctuations, leading to conservation of the 'Noether charge' Q in Matsubara time. Due to self-consistently arising local minimum of their potential energy at finite amplitude of the density fluctuations, the Q-balls provide greater binding energy of fermions into local/Cooper pairs relative to the usual Frohlich mechanism of exchange with infinitesimal lattice/charge/spin quasiparticles. We show that around some temperature T^* the Q-balls arise with a finite density of superconducting condensate inside them. The Q-balls expand their sizes to infinity at superconducting transition temperature T_c. The fermionic spectral gap inside the Q-balls arises in the vicinity of the 'nested' regions of the bare Fermi surface. Solutions are found analytically from the Eliashberg equations with the 'nesting' wave vectors connecting 'hot spots' in the Brillouin zone. The experimental 'Uemura plot' of the linear dependence of T_c on superconducting density n_s in high-T_c superconducting compounds follows naturally from the proposed theory.

Keywords: cooper-pairing 'glue'; Euclidean Q-balls; Eliashberg equations; 'nesting'; high-temperature superconductivity

Citation: Mukhin, S. Euclidean Q-Balls of Fluctuating SDW/CDW in the 'Nested' Hubbard Model of High-T_c Superconductors as the Origin of Pseudogap and Superconducting Behaviors. *Condens. Matter* **2022**, *7*, 31. https://doi.org/10.3390/condmat7020031

Academic Editor: Andrea Perali

Received: 6 February 2022
Accepted: 26 March 2022
Published: 31 March 2022

1. Introduction

We propose here a theory of Euclidean Q-ball phase of high-T_c superconductors in the 'nested' Hubbard model that may explain both the high-T_c superconductivity, as well as the 'pseudo gap' phase that precedes it. Namely, it is demonstrated analytically that Euclidean action of the strongly correlated electron system may possess stable saddle-point configurations in the form of finite size bubbles (Q-balls) with superconducting density fluctuations coupled to oscillating in Matsubara time fluctuations of spin or charge. This result is obtained via a self-consistent solution of the Eliashberg equations in combination with the condition of vanishing the first variational derivative of the effective Euclidean action with respect to an amplitude of the spin-/charge fluctuations; see Sections 4 and 5. The presented Q-balls picture is reminiscent of the famous Q-balls formation in the supersymmetric standard model, where the Noether charge responsible for baryon number conservation is associated with the U(1) symmetry of the squarks field [1,2]. Here, we found that near some temperature T^* the leading collective spin-/charge fluctuations acquire a form of finite volume Q-balls filled with Cooper/local-pair condensates. The phase of the dominating Fourier component of the Q-ball spin-/charge density fluctuations rotates with bosonic frequency in Matsubara time and causes local/Cooper pairing. Simultaneously, the Q-ball potential energy possesses a local minimum at a finite value of the modulus of this Fourier

component. It is demonstrated that the 'gas' of Q-balls arises near some temperature T^* as a 1st order phase transition. This mechanism of local/Cooper pairing differs from the usual Frohlich mechanism of exchange with infinitesimal lattice/charge/spin quasiparticles in e.g., phonon- or spin–fermion coupling models considered for high-T_c cuprates [3] and underlying t–J–U Hubbard models reviewed in [4–6]. The superconducting transition in the Q-ball system happens at some temperature T_c, where the Q-balls energy crosses zero and becomes negative, thus making the Q-ball volume infinite. At couplings stronger then some critical value κ^* found below, another scenario of superconducting transition is possible, when Cooper-/local pairs percolate between Q-balls forming an infinite superconducting cluster. The plan of the article is as follows: in Section 1, an effective U(1) symmetric Euclidean model of the SDW/CDW fluctuations described by a scalar amplitude field is outlined and the condition for the Q-ball emergence is derived. Section 2 contains derivation of the effective potential energy of the SDW/CDW fluctuations, induced by formation of a local superconducting condensate inside the Q-balls. The local superconducting 'pseudo gap' inside a Q-ball is self-consistently derived from the Eliashberg like equation that acquires the form of the Mathieu equation with the Matsubara time as a coordinate, while the propagator of the semiclassical SDW/CDW fluctuations plays the role of the periodic potential. In Section 3, the T^* and T_c temperatures are expressed in analytic form as functions of the spin/charge–fermion coupling constant, density of the 'nested' states, and short-range coherence length of the spin-/charge density waves in the strongly correlated electron system. Finally, a linear dependence of T_c on the superconducting density n_s is derived theoretically and demonstrates qualitative correspondence with the famous Uemura plot for high-T_c superconductors [7]. Possible applications of the presented theory for description of the other properties of high-T_c cuprates are discussed in Conclusions.

2. Effective Model

We consider a simplest model Euclidean action S_M with a scalar complex field $M(\tau, \mathbf{r})$ related with spin-/charge- density fluctuations :

$$S_M = \int_0^\beta \int_V d\tau d^D\mathbf{r} \frac{1}{g}\Big\{|\partial_\tau M|^2 + s^2|\partial_{\mathbf{r}} M|^2 + \mu_0^2|M|^2 + gU_f(|M|)\Big\},\ M \equiv M(\tau, \mathbf{r}) \qquad (1)$$

where $M(\tau + 1/T, \mathbf{r}) = M(\tau, \mathbf{r})$ is a periodic function of Matsubara time at finite temperature T [8], s is bare propagation velocity, and correlation length ξ of the fluctuations is defined by the 'mass' term $\mu_0^2/s^2 \sim 1/\xi^2$. The last term contains effective potential $U_f(|M|)$ that depends on the field modulus $|M|$, and the explicit expression for U_f is derived below by integrating out superconducting fluctuations, which are found self-consistently from an Eliashberg like equation in the 'nested' Hubbard model with spin-/charge–fermion interactions, see Equation (15). The model (1) is $U(1)$ invariant under the global phase rotation ϕ: $M \to Me^{i\phi}$. Hence, corresponding 'Noether charge' is conserved along the Matsubara time axis. The 'Noether charge' conservation makes possible Matsubara time periodic, finite volume Q-ball semiclassical solutions that otherwise would be banned in D > 2 by a Derrick theorem [9] in the static case. Previously Q-balls were introduced by Coleman [1] for Minkowski space in QCD, and have been classified as non-topological solitons [2]. As shown below, the Euclidean Q-balls describe stable semiclassical short-range charge/spin ordering fluctuations of finite energy that appear at finite temperatures near some temperature T^* found below. The fermionic spectral gap inside Euclidean Q-balls arises in the vicinity of the 'nested' regions of the bare Fermi surface (corresponding to the antinodal points of the cuprates Fermi-surface) and scales with the local superconducting density inside Q-balls. Hence, T^* defines temperature of a phase transition into the 'pseudo gap' phase, as was proposed previously [10].

Consider now time-dependent phase shift: $\phi = \Omega\tau$, with frequency $\Omega = 2\pi nT$ that satisfies Matsubara time periodicity. Then, the corresponding conserved 'Noether charge'

is found readily. First, one defines $D+1$-dimensional 'current density' $\{j_\tau, \vec{j}\}$ of the scalar field $M(\tau, \mathbf{r})$:

$$j_\alpha = \frac{i}{2}\{M^*(\tau,\mathbf{r})\partial_\alpha M(\tau,\mathbf{r}) - M(\tau,\mathbf{r})\partial_\alpha M^*(\tau,\mathbf{r})\},\ \alpha = \tau, \mathbf{r}. \tag{2}$$

Next, Euclidean trajectories of the field, defined by 'classical' equations of motion, are considered:

$$\frac{\delta S_M}{\delta M^*(\tau,\mathbf{r})} = -\partial_\tau^2 M(\tau,\mathbf{r}) - s^2 \sum_{\alpha=\mathbf{r}} \partial_\alpha^2 M(\tau,\mathbf{r}) + \mu_0^2 M(\tau,\mathbf{r}) + gM(\tau,\mathbf{r})\frac{\partial U_f}{\partial |M(\tau,\mathbf{r})|^2} = 0. \tag{3}$$

Using Equations (2) and (3), it is straightforward to prove the following relation:

$$\frac{\partial}{\partial\tau}\int_V j_\tau d^D\mathbf{r} = -s^2\int_V div\vec{j}\, d^D\mathbf{r} = -s^2\oint_{S(V)}\vec{j}\cdot d\vec{S}\,, \tag{4}$$

where the last integral in Equation (4) is taken over the surface S of the volume V due to the Gauss theorem. Hence, for the non-topological field configurations that occupy finite volume V, i.e., $M(\tau, \mathbf{r}\notin V) \equiv 0$, one finds:

$$\frac{\partial}{\partial\tau}\int_V j_\tau d^D\mathbf{r} = -s^2\oint_{S(V)}\vec{j}\cdot d\vec{S} = 0\,, \tag{5}$$

and, in turn, conserved 'Noether charge' Q equals:

$$Q = \int_V j_\tau d^D\mathbf{r} = \Omega M(\tau)^2 V\,, \tag{6}$$

where we have approximated the 'Q-ball' field configuration with a step function $\Theta(\mathbf{r})$:

$$M(\tau,\mathbf{r}) = e^{-i\Omega\tau}M\Theta\{\mathbf{r}\}\,;\quad \Theta(\mathbf{r}) \equiv \begin{cases} 1;\ \mathbf{r}\in V; \\ 0;\ \mathbf{r}\notin V. \end{cases} \tag{7}$$

In general, to find equilibrium volume of the Q-ball, one has to minimise the action S_M with respect to V under the conserved 'charge' Q defined by Equation (6). First, we do this in the step function approximation above, Equation (7). In this case, one finds action S_M using Equations (1) and (6), and neglecting the boundary contribution $\propto \int |\partial_\mathbf{r} M(\tau,\mathbf{r})|^2$:

$$S_M = V\frac{1}{gT}\Big\{[\Omega^2+\mu_0^2]M^2 + gU_f\Big\} = \frac{1}{gT}\Big\{\frac{Q^2}{VM^2} + V[\mu_0^2M^2 + gU_f]\Big\}. \tag{8}$$

Minimising Euclidian action of the Q-ball in Equation (8) with respect to volume V, one finds:

$$\frac{\partial S_M}{\partial V} = \frac{1}{gT}\Big\{-\frac{Q^2}{V^2M^2} + [\mu_0^2M^2 + gU_f(M^2)]\Big\} = 0. \tag{9}$$

Solving Equation (9), one finds equilibrium volume V_Q of the Q-ball and its energy E_Q:

$$V_Q = \frac{Q}{M\sqrt{\mu_0^2M^2 + gU_f(M^2)}}\,. \tag{10}$$

Substituting Equation (10) into Equation (8), one finds:

$$E_Q = TS_M^{min} = \frac{2Q\sqrt{\mu_0^2M^2 + gU_f(M^2)}}{gM} = \frac{2Q\Omega}{g}, \tag{11}$$

where the last equality follows directly after substitution of expression V_Q from Equation (10) into Equation (6). Since Q cancels in Equation (11), the following self-consistency equation follows:

$$\Omega = \frac{\sqrt{\mu_0^2 M^2 + g U_f(M^2)}}{M}. \tag{12}$$

In a more careful procedure that follows below, one uses saddle-point equation (3) for Euclidean action that provides coordinate dependence of $M(\tau, \mathbf{r})$. For this purpose, one has to add to the action S_M an extra term with the Lagrange multiplier that takes care of the 'charge' Q conservation:

$$S_M = \int_0^\beta \int_V d\tau d^D\mathbf{r} \frac{1}{g}\Big\{ |\partial_\tau M|^2 + s^2 |\partial_\mathbf{r} M|^2 + \mu_0^2 |M|^2 + g U_f(|M|^2) + i\mu\{M^*(\tau,\mathbf{r})\partial_\tau M(\tau,\mathbf{r}) - M(\tau,\mathbf{r})\partial_\tau M^*(\tau,\mathbf{r})\}\Big\},\ M \equiv M(\tau,\mathbf{r}) \tag{13}$$

It is easy to find that the value of the 'chemical potential' μ should be $\mu = -\Omega$, in order to recover from Equation (13) the approximate self-consistency Equation (12) in the step-function approximation Equation (7). Then, substituting S_M from Equation (13) into dynamic Equation (3) in Euclidean space-time and, using for the time-dependence $M(\tau, \mathbf{r}) \propto \exp\{-i\Omega t\}$, one finally obtains the coordinate dependent self consistency equation, to be solved below:

$$-s^2 \Delta M + g \partial U_f / \partial M + (\mu_0^2 - \Omega^2) M = 0, \tag{14}$$

compare [1]. A Euclidean Q-ball described by Equations (6), (12), and (14) differs from the Q-ball in Minkowski space [1]: at fixed temperature T, a choice of the values of the Matsubara frequencies $\Omega = 2\pi n T$ in Euclidean space-time is discrete due to integer n and starts from $\Omega = 2\pi T$, contrary to a continuum of the frequency values in the Minkowski space-time. Hence, the highest temperature T^*, at which Equation (12) possesses a solution, would be for $n = 1$, and would manifest a transition into a Q-ball 'gas' phase, corresponding to a pseudogap phase, as will be shown below. Next, at temperature $T_c < T^*$, the Q-ball becomes infinite according to the solution of Equation (14), and a phase transition into bulk superconducting phase takes place. One has to derive an explicit expression for the effective energy $U_f(M)$ in order to explore the phase diagram of the Q-balls 'gas' in the next sections.

3. Free Energy of the Cooper-Pairing Fluctuations inside the Q-Balls

Here, we derive an effective potential $U_f(|M(\mathbf{r})|)$, the density of the free energy decrease $\Delta\Omega_s$ being due to superconducting fluctuations. Consider a simple model of fermions on a square lattice that are linearly coupled to the dominant Q-ball type charge- or spin density fluctuations that obey Equation (3), and possess amplitude $M(\tau, \mathbf{r}) \equiv e^{-i\Omega\tau} M(\mathbf{r})$ with wave vectors Q_{CDW} or Q_{SDW}, respectively. In what follows, we accept generalised notation Q_{DW} for both cases. Thus, the fermionic part of the Euclidean action S_f takes the form:

$$S_f = \frac{1}{V}\int_0^\beta d\tau \int_V d^D\mathbf{r} \sum_{\mathbf{q},\sigma} \Big[c^+_{\mathbf{q}\sigma}(\partial_\tau + \varepsilon_q) c_{\mathbf{q},\sigma} + \Big(c^+_{\mathbf{q}+\mathbf{Q_{DW}},\sigma} M(\tau,\mathbf{r}) \sigma c_{\mathbf{q},\sigma} + H.c. \Big) \Big], \tag{15}$$

and antiferromagnetic fluctuations are considered below for definiteness using standard Hamiltonian [3] with spin–fermion coupling. Then, the Matsubara time periodic complex amplitude $M(\tau, \mathbf{r})$, considered in general in the preceding section, acquires a particular meaning of the amplitude of the SDW fluctuation, with the fast space oscillations on the

lattice variable $\mathbf{r}$ being characterised by a wave-vector Q_{DW}, and slow variations happen on the scale of the correlation length or Q-ball radius:

$$M_{\tau,\mathbf{r}} = M(\tau,\mathbf{r})e^{i\mathbf{Q_{DW}}\cdot\mathbf{r}} + M(\tau,\mathbf{r})^* e^{-i\mathbf{Q_{DW}}\cdot\mathbf{r}},$$
$$M(\tau,\mathbf{r}) \equiv |M(\tau,\mathbf{r})|e^{-i\Omega\tau},\ \Omega = 2\pi nT,\ n = 1,2,... \quad (16)$$

Here, Ω is bosonic Matsubara frequency, and σ in Equation (15) is a local z-axis projection of the fermionic spin assumed to be collinear with the direction of the spin density inside a Q-ball. Actually, spin–fermion coupling action (15) could be obtained after decoupling of the on-site inter-fermion repulsive U-term: $Un_{i,\uparrow}n_{i,\downarrow}$ in the Hubbard Hamiltonian via auxiliary Hubbard–Stratonovich field $M(r,\tau)$, see e.g., [10,11]. Then, before renormalisations, the constant g in Equation (1) is formally inferred from the term $\mu_0^2|M|^2$ and Equation (15): $g \sim \mathrm{U}\mu_0^2 \sim 10^{-2}$ eV^3, where the last estimate is based on the value of U$\sim$ 4–6 eV for the single band Hubbard model [4,6], and on results of neutron measurements, $\mu_0 \sim$ 100–200 meV, of the spin-wave excitations in doped high-T_c cuprates [12,13]. An effective theory is then obtained by formally integrating out fermions, assuming that they undergo local Cooper pairing fluctuations with emerging Bogoliubov anomalous averages $< c_{\mathbf{q},\sigma}c_{-\mathbf{q},-\sigma} >$, $< c^+_{\mathbf{q},\sigma}c^+_{-\mathbf{q},-\sigma} >$ entering the diagrammatic expansion of the free energy Ω_s [10]:

$$VU_f(|M(\tau,\mathbf{r})|) = \Delta\Omega_s = -T\ln\frac{Tr\left\{e^{-\int_0^\beta H_{int}(\tau)d\tau}\mathcal{G}(0)\right\}}{Tr\{\mathcal{G}(0)\}} \equiv \Omega_s - \Omega_0;\ \mathcal{G}(0) \equiv e^{-\beta H_0}; \quad (17)$$

$$H_{int} = \frac{1}{V}\int_V d^D\mathbf{r}\sum_{\mathbf{q},\sigma}\left(c^+_{\mathbf{q}+\mathbf{Q_{DW}},\sigma}M(\tau,\mathbf{r})\sigma c_{\mathbf{q},\sigma} + H.c.\right), \quad (18)$$

where H_0 is inferred from the first and H_{int} from the second term in the sum in (15) respectively. Next, we multiply Hamiltonian H_{int} in (18) with a dimensionless amplitude $0 < \alpha < 1$, as a formal variable coupling strength in the spin–fermion interaction, and calculate the free energy derivative in accordance with the usual prescription [8]:

$$\frac{\partial\Delta\Omega_s}{\partial\alpha} = T\int_0^\beta\left\langle\frac{\partial H_{int}(\tau)}{\partial\alpha}\right\rangle d\tau = -\frac{T}{\alpha}\int_0^\beta\int_0^\beta d\tau d\tau_1\langle H_{int}(\tau)H_{int}(\tau_1)\rangle =$$
$$-\frac{1}{\alpha}|M|^2T\sum_{\omega,\mathbf{p},\sigma}\sigma\bar{\sigma}\overline{F}_{\sigma,\bar{\sigma}}(\omega,\mathbf{p})F_{\bar{\sigma},\sigma}(\omega-\Omega,\mathbf{p}-\mathbf{Q_{DW}})\alpha^2\,, \quad (19)$$

where we have neglected slow dependence of the modulus of the SDW amplitude $|M|$ on $\tau,\mathbf{r}$ in the step function approximation (7). The loop of Gor'kov anomalous functions $F^\dagger, F$ connected with the 'gluon' line $D(\tau-\tau') \sim M(\tau')^*\cdot M(\tau)$, depends now on parameter α. The amplitudes M in Equation (16) of spin-/charge density fluctuations obey 'classical' equations of motion Equation (3) that extremize Euclidean action. In the case when wave vector Q_{DW} connects 'nested' points on the Fermi surface belonging to the regions with opposite signs of the d-wave superconducting order parameter, the following algebraic relations hold for the dispersion and self-energy functions [10]:

$$\varepsilon_{p-Q_{DW}} = -\varepsilon_p \equiv -\varepsilon;\quad \Sigma_{2p-Q_{DW},\sigma} = -\Sigma_{2p,\sigma};\quad \Sigma^*_{1p,\sigma}(\omega) \equiv \Sigma_{1,-p,\bar{\sigma}}(-\omega)\,; \quad (20)$$

$$F_{p,\sigma}(\omega) = \frac{-\Sigma_{2p,\sigma}}{|i\omega-\varepsilon_p-\Sigma_{1p,\sigma}(\omega)|^2+|\Sigma_{2p,\sigma}(\omega)|^2},\quad \omega = \pi(2n+1)T;\quad n = 0,\pm1,\ldots \quad (21)$$

In what follows, we neglect renormalisations [10] entering via self-energy $\Sigma_{1p,\sigma}(\varepsilon,\omega)$ in denominator in Equation (21) for the anomalous fermionic Green function $F_{p,\sigma}(\omega)$, and use d-wave symmetric behaviour of superconducting order parameter $\Sigma_{2p-Q_{DW},\sigma} = -\Sigma_{2p,\sigma}$

represented by the self-energy function $\Sigma_{2p,\sigma}$. The latter is approximated with a parabolic function of bare fermionic dispersion ε_p in the vicinity of the Fermi energy:

$$|\Sigma_{2p,\sigma}(\omega)|^2 = g_0^2 - \varepsilon_p^2 . \tag{22}$$

Simultaneously, the fermionic spectrum inside the Q-ball acquires the form, see Figure 1:

$$E_p = \begin{cases} g_0; \ |\varepsilon_p| \leq \min\{g_0, \varepsilon_0\}; \\ \varepsilon_p; \ |\varepsilon_p| > \min\{g_0, \varepsilon_0\}. \end{cases} \tag{23}$$

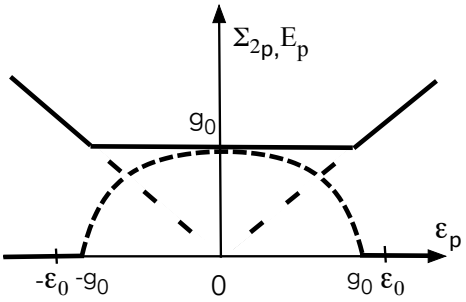

Figure 1. Anomalous self-energy $\Sigma_{2p,\sigma}$ (short-dashed line) and fermionic dispersion E_p (solid line) as a function of bare fermionic dispersion ε_p in the vicinity of the Fermi-level $\mu_f = 0$ near the 'nested'/anti-nodal points of the bare Fermi surface inside a Q-ball with local superconducting (pseudo)gap g_0, see Equations (22) and (23).

Hence, the superconducting (pseudo)gap g_0 in the spectrum of fermions populating the Q-balls arises under such a scheme only in the vicinities of the antinodal points. A problem of creation of the Fermi arcs is, in principle, treatable in the presented Q-ball gas picture but demands elaboration of the self consistency equation for momenta p also outside the antinodal points. An explicit 2D momentum dependence of the superconducting gap is not considered in the simplified picture used in the present work and will be considered elsewhere. The consequence of the latter approximation is discussed below in Section 6.1. Now, substituting expressions in Equations (20) and (21) into Equation (19), one finds:

$$\frac{\partial \Omega_s}{\partial \alpha} = -TVR\alpha; \quad R = \frac{4M^2 \nu g_0 \varepsilon_0}{3T(\Omega^2 + 4g_0^2)} \tanh\frac{g_0}{2T} \tanh\frac{g_0}{\varepsilon_0} . \tag{24}$$

Here, expression for R in Equation (24) is obtained after summation over fermionic frequency $\omega = \pi(2n+1)$ in Equation (19), while neglecting ω-dependence of the self-energy $\Sigma_{2p,\sigma}(\omega) \approx \Sigma_{2p,\sigma}(0)$, since summation in Equation (19) over ω is quickly convergent. Summation over momenta $\mathbf{p}$ in Equation (19) is substituted by integration over ε_p (counted from the Fermi level μ_f) over bare density of 'nested' states $\nu(\varepsilon_p)$ approximated as:

$$\nu(\varepsilon_p) = \begin{cases} \nu; \ |\varepsilon_p| \leq \varepsilon_0; \\ 0; \ |\varepsilon_p| > \varepsilon_0. \end{cases} \tag{25}$$

Since $|\Sigma_{2p,\sigma}(\omega)|^2 = g_0^2 - \varepsilon_p^2 \geq 0$, see Figure 1, differs from zero inside an interval: $-g_0 \leq \varepsilon_p \leq g_0$, the product $\nu g_0 \varepsilon_0 \tanh g_0/\varepsilon_0$ in Equation (24) interpolates between the cases $g_0 > \varepsilon_0$ and $g_0 < \varepsilon_0$. Now, one has to bear in mind that $g_0 = g_0(\alpha)$, and, hence, $R(\alpha)$ defined in Equation (24) depends on the integration variable α introduced above. To complete derivation of the effective potential $U_f(|M(\tau, \mathbf{r})|)$, one has to find constant g_0^2 entering expression for R. The local 'superconducting pseudogap' g_0 is found from the self-consistency condition derived below, see also [10]. Importantly, the final expression

of the kind obtained in Equation (24) appears also in the case when charge fluctuations instead of spin fluctuations couple to the fermions via interaction Hamiltonian:

$$H_{int}^{CDW} = \frac{1}{V}\int_V d^D\mathbf{r}\sum_{\mathbf{q},\sigma}\left(c^+_{\mathbf{q}+\mathbf{Q_{DW}},\sigma}M(\tau,\mathbf{r})c_{\mathbf{q},\sigma} + H.c.\right), \tag{26}$$

where σ spin factor is missing in the charge–fermion coupling vertex c^+Mc. This would, in turn, lead to the absence of the factor $\sigma\bar{\sigma} = -1$ in Equation (19). Hence, in order to keep $U_f < 0$ (the driving force of the Q-ball transition), one has to compensate for this sign change. For this, it is necessary to change the sign of the Green's functions product $\overline{F}_{\sigma,\bar{\sigma}}(\omega,\mathbf{p})F_{\bar{\sigma},\sigma}(\omega-\Omega,\mathbf{p}-\mathbf{Q_{DW}})$ in Equation (19). Then, allowing for the structure of the Gor'kov's anomalous Green's function in Equation (21), one concludes that, in order to change the sign of the Green's functions product, one has to change the relation between the signs of superconducting order parameters in the points connected by the 'nesting' wave vector Q_{CDW}. Hence, in case of CDW-mediated pairing [14,15], the 'nesting' wave vector should couple points with the same sign of a superconducting order parameter corresponding to the s-wave coupling [3]: $\Sigma_{2p-Q_{CDW},\sigma} = \Sigma_{2p,\sigma}$. Such choice then changes the sign of the product $\overline{F}_{\sigma,\bar{\sigma}}(\omega,\mathbf{p})F_{\bar{\sigma},\sigma}(\omega-\Omega,\mathbf{p}-\mathbf{Q_{DW}})$ in the free energy integral in Equation (19) just compensating for the absence of the factor $\sigma\bar{\sigma} = -1$, and, hence, keeping intact the major condition : $U_f < 0$.

4. Eliashberg Equations and Bound States along the Axis of Matsubara Time

Now, using definition of the anomalous fermionic Green's function $F_{p,\sigma}(\omega)$ in Equation (21), one obtains the Eliashberg equation for the self-energy $\Sigma_{2p,\sigma}(\omega)$ [10,16] in the form:

$$\Sigma_{2p,\sigma}(\omega) = \frac{-T\mathcal{D}_{Q_{DW}}(\Omega)\Sigma_{2,p-Q_{DW},\sigma}(\omega-\Omega)}{|i(\omega-\Omega)-\varepsilon_{p-Q_{DW}}-\Sigma_{1p-Q_{DW},\sigma}(\omega-\Omega)|^2+|\Sigma_{2p-Q_{DW},\sigma}(\omega-\Omega)|^2} \tag{27}$$

$$\mathcal{D}_{Q_{DW}}(\Omega) \equiv \frac{M^2}{T} \tag{28}$$

where expression in Equation (28) for the 'glue boson' propagator is inferred from the definition of the considered above 'classical' Q-ball field $M(\tau,\mathbf{r})$, as defined in Equations (7) and (16), and monochromaticity of the 'glue boson' propagator is taken into account, thus transforming Equation (27) into the algebraic. It is easy to compare Equations (27) and (21) and obtain readily an equation for the anomalous Green function $F_{p,\sigma}(\omega)$ in the closed form (compare [10]):

$$F_{p,\sigma}(\omega) = -\Sigma_{2p,\sigma}(\omega)K_p(\omega) = -K_p(\omega)\left[\mathcal{D}_{Q_{DW}}(\Omega)F_{p-Q_{DW},\sigma}(\omega-\Omega)\right], \tag{29}$$

$$K_p(\omega) = \left\{|i\omega-\varepsilon_p-\Sigma_{1p,\sigma}(\omega)|^2+|\Sigma_{2p,\sigma}(\omega)|^2\right\}^{-1} \approx \left\{\omega^2+\varepsilon_p^2+|\Sigma_{2p,\sigma}(\omega)|^2\right\}^{-1}. \tag{30}$$

Now, after applying inverse Fourier transform to both sides of Equation (29), one finds:

$$F_{p,\sigma}(\tau) = \int_0^{1/T} K_p(\tau-\tau')\mathcal{D}_{Q_{DW}}(\tau')F_{p,\sigma}(\tau')d\tau'. \tag{31}$$

When writing Equation (31), the d-wave symmetry of the self-energy: $\Sigma_{2p-Q_{DW},\sigma} = -\Sigma_{2p,\sigma}$ was taken into account. Approximating denominator of $K_p(\omega)$ as indicated in Equation (30), one finds:

$$K_p(\tau) = T\sum_\omega \frac{e^{-i\omega\tau}}{|i\omega-\varepsilon_p-\Sigma_{1p,\sigma}(\omega)|^2+|\Sigma_{2p,\sigma}(\omega)|^2} \approx \frac{\sinh\left[g_0\left(\frac{1}{2T}-|\tau|\right)\right]}{2g_0\cosh\left(\frac{g_0}{2T}\right)}, \tag{32}$$

where g_0 is defined in Equation (22). It is straightforward to check that (32) possesses the following property:

$$\partial_\tau^2 K_p(\tau) = g_0^2 K_p(\tau) - \delta(\tau), \tag{33}$$

Hence, using the above relation (33) and differentiating Equation (31) twice over τ, we obtain the following Schrödinger like equation for the wave function $F_{p,\sigma}(\tau)$ of the local/Cooper pair along the Matsubara time axis τ:

$$-\partial_\tau^2 F_{p,\sigma}(\tau) - \mathcal{D}_{Q_{DW}}(\tau) F_{p,\sigma}(\tau) = -g_0^2 F_{p,\sigma}(\tau). \tag{34}$$

Using now Equation (28) for the 'glue boson' propagator $\mathcal{D}_{Q_{DW}}$, one finds that Gor'kov's anomalous Green function $F_{p,\sigma}(\tau)$ of the superconducting condensate inside the Q-ball obeys the Mathieu equation [17]:

$$\partial_\tau^2 F_{p,\sigma}(\tau) + \left(2M^2 \cos(\Omega\tau) - g_0^2\right) F_{p,\sigma}(\tau) = 0, \quad F_{p,\sigma}\left(\tau + \frac{1}{T}\right) = -F_{p,\sigma}(\tau)\,, \tag{35}$$

where the anti-periodicity condition of the fermionic Green function $F_{p,\sigma}(\tau)$ [8] is explicitly indicated. Since $\Omega = 2\pi n T$ in (35) is bosonic Matsubara frequency, the anti-periodicity condition in Equation (35) imposes a self-consistency relation between the SDW amplitude M and the 'superconducting pseudogap' g_0, which is a necessary condition for the existence of solution $F_{p,\sigma}(\tau)$. To find this self-consistency relation in approximate analytic form, one may consider Equation (35) as Schrödinger equation and substitute potential $V(\tau) = -2M^2 \cos(\Omega\tau)$ with rectangular potential of the amplitude $2M^2$ in the interval $-1/2T \leq \tau \leq 1/2T$, looking for the odd bound state inside this potential well. Then, it is known that such a potential well contains the second lowest possible eigenvalue $-g_0^2$ just crossing zero of energy under the condition [18]:

$$g_0^2 \approx 2M(M-\Omega) \rightarrow g_0^2(\alpha) \approx 2M\alpha(M\alpha - \Omega)\,, \tag{36}$$

where, at the last step, an amplitude M is substituted with αM according to the definition of the formal variable coupling strength parameter α in Equation (19). Then, after substitution of solution from Equation (36) into Equation (24), one finds the following expression for the function $R(\alpha)$:

$$\alpha^2 R(\alpha) = \frac{4M^2 \nu \varepsilon_0 \alpha^2 \sqrt{2\alpha M(\alpha M - \Omega)}}{3T(\Omega^2 + 8\alpha M(\alpha M - \Omega))} \tanh \frac{\sqrt{2\alpha M(\alpha M - \Omega)}}{\varepsilon_0} \tanh \frac{\sqrt{2\alpha M(\alpha M - \Omega)}}{2T}. \tag{37}$$

Now, using Equation (24), one obtains the following expression for the pairing-induced effective potential energy of SDW/CDW field that enters a Q-ball self-consistency condition in Equation (12):

$$U_{eff}(M) = \mu_0^2 M^2 + g U_f = \mu_0^2 M^2 - \frac{4g\nu\varepsilon_0\Omega}{3} I\left(\frac{M}{\Omega}\right)\,,\ M \equiv |M(\tau)| \tag{38}$$

$$I\left(\frac{M}{\Omega}\right) = \int_1^{M/\Omega} d\alpha \frac{\alpha\sqrt{2\alpha(\alpha-1)}}{(1+8\alpha(\alpha-1))} \tanh \frac{\sqrt{2\alpha(\alpha-1)}\Omega}{\varepsilon_0} \tanh \frac{\sqrt{2\alpha(\alpha-1)}\Omega}{2T}. \tag{39}$$

Figure 2 contains plots of $U_{eff}(M)$ at different temperatures, manifesting characteristic 'Q-ball local minimum' [1]: near T^* temperature, where the Q-ball phase has emerged, and, close to T_c, at which the Q-ball volume becomes infinite and bulk superconductivity sets in.

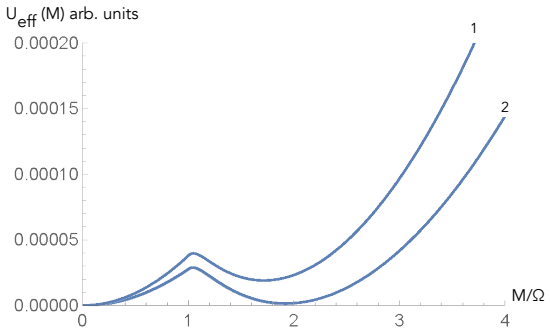

Figure 2. Effective potential energy U_{eff} of the SDW/CDW fluctuation as a function of the amplitude M weighted by Matsubara frequency $\Omega = 2\pi nT$ at two different temperatures $T_1 = T^*$—curve 1, and $T_2 = T_c$—curve 2, see text.

Then, it is straightforward to substitute $U_{eff}(M)$ from Equation (38) into self-consistency Equation (12) rewritten using a definition of 'shifted' by $-M^2\Omega^2$ potential energy U_{eff}:

$$\tilde{U}_{eff} \equiv (\mu_0^2 - \Omega^2)M^2 - \frac{4\Omega g\nu\varepsilon_0}{3} I\left(\frac{M}{\Omega}\right) = 0. \tag{40}$$

The contour plots of Equation (40) in the plane $\{M/\Omega, \Omega\}$ are represented in Figure 3 for different ranges of the coupling strength.

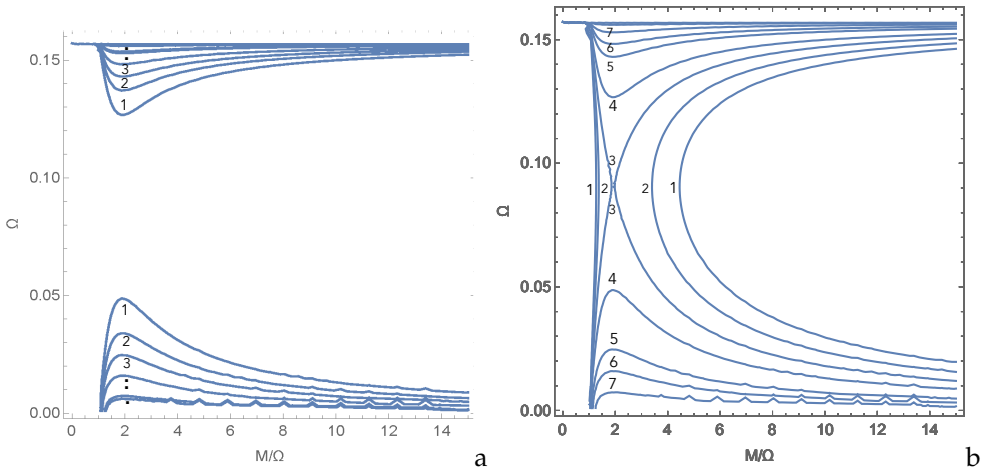

Figure 3. The contour plots of self-consistency Equation (40) in the plane $\{M/\Omega, \Omega\}$ are presented: (**a**) the numerated 1–3-... curves are plotted for different values of parameter $\kappa \equiv 4g\nu\varepsilon_0$ in the 'weak coupling' interval of values $\kappa < \kappa^*$, see text after Equation (42); (**b**) same as (**a**), but with added curves numerated 1–3 in the interval of 'strong' couplings $\kappa \geq \kappa^*$, and with curves numerated 4–7 in the 'weak coupling' interval $\kappa < \kappa^*$ kept for convenience of comparison.

It will be demonstrated in the next section that Figure 3 signifies the following: (1) at weak couplings, the pseudogap phase terminates at temperatures T^* that are much higher than the temperatures T_c of a bulk superconducting transition; (2) there is some limiting coupling strength, at which T^* touches T_c; (3) at even stronger couplings, the expression on the l.h.s of Equation (40) never touches zero at its minimum but always crosses zero at two different values of M/Ω, of which one approaches limit $M/\Omega = 1$ of zero superconducting density, and the opposite one goes to 'infinity'. It is also noticeable from Figure 3 that local minima of $\tilde{U}_{eff}$, which obey Equation (40) for the different coupling strengths, are located nearly at one and the same coordinate along the M/Ω axis, i.e., at fixed ratio: $M/\Omega \approx 2$.

Using this fact, one obtains from Equation (40) the following approximate cubic equation for Ω that provides the $T^*(\kappa)$ and $T_c(\kappa)$ boundaries in the phase diagram:

$$(\mu_0^2 - \Omega^2) - c\frac{4g\nu\varepsilon_0}{3\Omega} = 0; \quad c = \left(\frac{\Omega}{M}\right)^2 I\left(\frac{M}{\Omega}\right)_{\frac{M}{\Omega}=2} \approx 0.01\,. \tag{41}$$

The value of $\kappa \equiv c\frac{4g\nu\varepsilon_0}{3}$, at which T^* meets T_c, and respective temperature T_0 are:

$$\kappa^* = \frac{2\mu_0^3}{3^{3/2}}\,;\; T_c = T^* = T_0 = \frac{\mu_0}{2\pi\sqrt{3}} \tag{42}$$

The phase diagram that follows from Equation (41) is plotted in Figure 4. To the right of the $T(\kappa)$ curve, i.e., for $\kappa > \kappa^*$, the 'pseudo-gap' and superconducting phases are not divided, the Q-balls possess finite radii and $M/\Omega \approx 1$, according to the coordinates of the 'vertical' contours in Figure 3b; hence, the superconducting density becomes small again: $g_0 = \sqrt{2M(M-\Omega)} \to 0$ together with the pseudogap, see Figure 1, and superconducting transition may acquire a percolative character due to Josephson tunneling between Q-balls forming infinite percolating clusters. The normal conductivity itself in the not superconducting (pseudogap) state above T^* has to be considered using a percolation approach for the electron current path that contains 'short-circuits' formed by finite size clusters of Q-balls possessing Josephson links between them, as well as resistive parts in the regions outside the Q-balls. This picture will be considered elsewhere and compared with the known properties of the 'strange metal' phase [19].

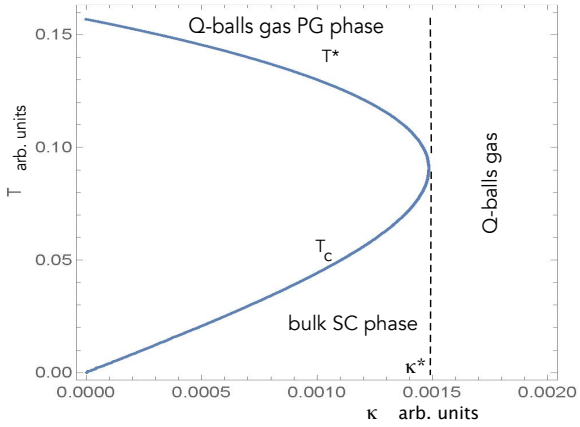

Figure 4. The phase diagram that follows from Equation (41), where $\kappa \equiv c\frac{4g\nu\varepsilon_0}{3}$, see text.

The phase diagram in Figure 4 obtained in the 2D plane {temperature, coupling constant} is actually in qualitative correspondence with the right half of the diagram for the stripe-phase bubbles formation experimentally found in the 2D plane {temperature, micro-strain ϵ in the CuO2 plane of all high-T_c cuprates}, see [20]. The other half is assumed to be possible to find by considering the percolative behaviour for the Cooper-pairs of the Q-balls gas. On the other hand, to calculate phase diagram in the plane {temperature, doping concentration}, one has to solve an extra microscopic problem to find a relation between the effective coupling constant κ and the doping concentration of holes. This is an interesting problem to be solved in the future.

5. The Q-Balls' Sizes

It is possible to understand the relation between the Q-balls radii R and the contour plots presented in Figure 3 by investigating a complete coordinate dependent Equation (14) for the Q-ball field M that minimises Euclidean action. Namely, using the definition of $\tilde{U}_{eff}$

in Equation (40) and representation of Laplacian operator in a spherically symmetric case, one rewrites Equation (14) in the equivalent form:

$$\frac{d^2M}{dr^2} = -\frac{2}{r}\frac{dM}{dr} - \frac{d\{-\tilde{U}_{eff}\}}{s^2 dM} \tag{43}$$

that formally coincides with a Newtonian equation of motion for a particle of unit mass in viscous environment moving in the potential $-\tilde{U}_{eff}/s^2$, where radius r plays the role of 'time' and fluctuation modulus M plays the role of 'coordinate', compare [1]. Neglecting 'damping' at large enough r, one finds an 'integral of motion':

$$\frac{1}{2}\left\{\frac{dM}{dr}\right\}^2 - \tilde{U}_{eff} = \tilde{E} = 0 \tag{44}$$

The integral of 'motion' $\tilde{E}$ is chosen to be zero taking into account finiteness of the Q-balls: $M(r >> R) = 0$. Finally, $\{\dot{M}^2\}/2$ plays the role of 'kinetic energy'. Then, consider the plots of the potential $-\tilde{U}_{eff}$ obtained using Equations (38) and (40), see Figure 5. It is straightforward to conclude from the conservation law (44) and Figure 5 that coordinate M of the 'particle' would take nearly 'infinite time' ($R \to \infty$) to reach point $M = 0$ when it starts close to the top of the potential at an 'initial time' ($r = 0$) that happens when the maximum of $-\tilde{U}_{eff}$ touches axis M/Ω. On the other hand, when $-\tilde{U}_{eff}$ crosses axis M/Ω at 'initial time' $r = 0$, it will take finite 'time' R to reach point $M(R) = 0$. Finally, when $-\tilde{U}_{eff}$ never crosses the axis M/Ω at any finite initial 'time' $r = 0$, the finite time travel is not possible, i.e., no Q-ball solution exists for the case of the lowest curves $\Omega = 0.1$; 0.11 in Figure 5a,b respectively.

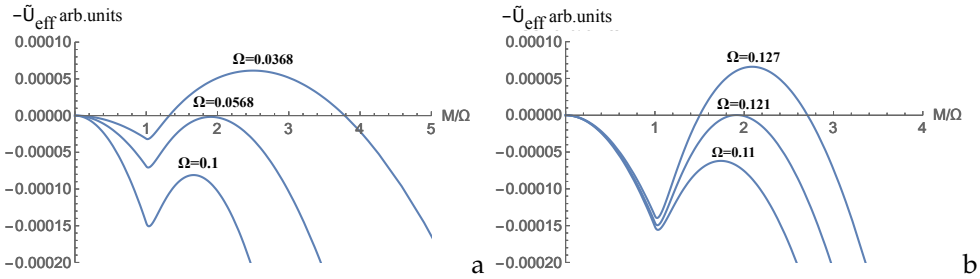

Figure 5. The plots of the potential energy $-\tilde{U}_{eff}$ for different values of Matsubara frequency $\Omega = 2\pi T$ at fixed coupling strength value κ corresponding to contour curves 4 in Figure 3b. (**a**) The set of curves in the superconducting domain $T \leq T_c$ in Figure 3; (**b**) the set of curves in the $T \geq T^*$ domain in Figure 3.

Finally, in order to distinguish different behaviours of the system when the radius of the Q-ball becomes infinite at $T = T_c$ and $T = T^*$, it is important to check the sign of the Q-balls potential energy U_{eff} given by Equation (38), (39) in the two temperature intervals. It is most simple to check using approximate Equation (41), from which it readily follows that $U_{eff} < 0$ when $T \leq T_c$, hence bulk superconductivity at $R \to \infty$ takes place, while $U_{eff} > 0$ when $T_c \leq T \leq T^*$, and, therefore, the probability of the Q-ball with $R \to \infty$ goes to zero; hence, no Q-ball phase is inside the loop $T_c(\kappa) - T^*(\kappa)$ in Figure 4.

6. The T_c vs. Superconducting Density N_s: The Uemura Plot

The above obtained solutions of the Q-ball self-consistency Equation (41) and Eliashberg Equation (36) allow one to calculate the density of the superconducting condensate inside the Q-balls represented by diagonal value of the Gor'kov Green's function F:

$$n_s = \frac{1}{V}\sum_p \left| T\sum_\omega F_p(\omega) \right|^2 = \frac{1}{V}\sum_p \left(\frac{\sqrt{g_0^2 - \varepsilon_p^2}}{2g_0} \tanh\frac{g_0}{2T} \right)^2 \tag{45}$$

where, in the last step, an expression for the self-energy Σ_2 from Equation (22) was used. One has to take into account an expression for the density of the fermionic 'nested' states Equation (25) in order to accomplish summation over momentum space in Equation (45), thus leading to the final result:

$$n_s = 2\int_0^{g_0} \nu \left(\frac{1}{2g_0} \tanh \frac{g_0}{2T} \sqrt{g_0^2 - \varepsilon^2} \right)^2 \Theta(\varepsilon_0 - \varepsilon)\, d\varepsilon \approx \frac{\nu\varepsilon_0}{2} \tanh^2 \frac{g_0}{2T} \tanh \frac{2g_0}{3\varepsilon_0} \tag{46}$$

where $\Theta(x)$ is Heaviside function, and the last factor extrapolates between the two cases $g_0 < \varepsilon_0$ and $g_0 > \varepsilon_0$. Now, it is straightforward to substitute in Equation (46) an expression for g_0 from the self-consistency Equation (36), and then use approximate relation $M = 2\Omega$, valid for points on T_c curve just above the superconducting transition, see Figure 4 :

$$g_0 = \sqrt{2M(M-\Omega)} \approx 2\Omega_c\,;\; n_s = \frac{\nu\varepsilon_0}{2} \tanh^2 \frac{2\Omega_c}{2T_c} \tanh \frac{2\Omega_c}{3\varepsilon_0} \approx \frac{\nu\varepsilon_0}{2} \tanh \frac{4\pi T_c}{3\varepsilon_0} \tag{47}$$

where one takes into account $\Omega_c \equiv 2\pi T_c$, leading to $\tanh \frac{2\Omega_c}{2T_c} = \tanh 2\pi \approx 1$. Expression (47) is remarkable: in the limit of relatively small transition temperatures $T_c \ll \varepsilon_0/\pi$, it produces linear dependence of superconducting T_c on the density n_s of the local Cooper-pair Bose-condensate in the Q-balls with the radius approaching infinity (bulk superconductivity transition):

$$n_s \approx \frac{2\pi\nu}{3} T_c\,. \tag{48}$$

Here, ν is the density of fermionic 'nested' states (e.g., in the antinodal regions of cuprates fermi-surface). Thus, Equation (48) may explain qualitatively the linear dependence of T_c on superconducting density n_s in high-T_c superconducting compounds found experimentally [7].

6.1. The Size of the Cooper-Pair Function

Using an expression for the anomalous Gor'kov Green function $F_p(\omega)$ from Equation (45), it is straightforward to evaluate the Cooper-pair 'size' inside a Q-ball by calculating coordinate dependence of the pair wave-function $\Psi(\mathbf{r})$:

$$\Psi(\mathbf{r} = \mathbf{r}_1 - \mathbf{r}_2) = F(\mathbf{r}_1, \mathbf{r}_2, \tau = 0) = T\sum_{p,\omega} F_p(\omega) \exp\{i\mathbf{pr}\} =$$

$$\frac{1}{2g_0} \tanh \frac{g_0}{2T} \sum_p \sqrt{g_0^2 - \varepsilon_p^2} \exp\{ip_x x\} \propto \frac{\pi g_0 \nu}{2} \tanh \frac{g_0}{2T} \cos(p_f x) \left(J_0(\frac{g_0 x}{v_f}) + \right.$$

$$\left. J_2(\frac{g_0 x}{v_f}) \right) \approx \frac{\pi g_0 \nu}{2} \tanh \frac{g_0}{2T} \cos(p_f x) \begin{cases} 1;\; x \ll v_f/g_0; \\ \dfrac{1}{(g_0 x/v_f)^{3/2}};\; x \gg v_f/g_0. \end{cases} \tag{49}$$

where J_0, J_2 are the Bessel functions of the first kind of order 0 and 2, respectively; the x-axis goes along the 'antinodal' direction of the 'nesting' wave-vector $\mathbf{Q}_{DW}$, and there is no dependence on the coordinate in the 'nodal' direction perpendicular to $\mathbf{Q}_{DW}$. Hence, in our rough approximation for the anomalous self-energy Σ_2 being non-zero only in the vicinity of the 'antinodal' points in Brillouin zone the 'shape' of the Cooper-pair is 'starfish' like: it is characterised by the length scale v_f/g_0 in the 'antinodal' direction, and by the Q-ball radius in the 'nodal' direction, in qualitative correspondence with experiment [21]. Substituting $g_0 \sim T^* \sim \mu_0$ according to Equation (42), one estimates the characteristic size scale along the 'antinodal' direction: $v_f/g_0 \sim v_f/\mu_0 \sim (v_f/s)\xi$, where ξ is correlation length of the spin-/charge fluctuation inside the Q-ball, see Equation (1). Power law decrease of the wave-function in Equation (49) formally indicating divergence of the pairs size has its

origin in the crude ansatz for the anomalous self-energy Σ_2 momentum dependence in Equation (22) mentioned after Equation (23).

7. Discussion

To summarise, a 'pairing glue' by exchange with coherent semiclassical fluctuations inside finite volume nontopological Euclidean solitons, Q-balls, is proposed as a mechanism of pseudogap phase and high temperature superconductivity in high-T_c cuprates. It is demonstrated that Euclidean Q-balls of semiclassical spin-/charge density-wave fluctuations that self-consistently support formation of local superconducting condensates can emerge as the 'smoking gun' of the pseudogap phase and high temperature superconductivity in strongly enough coupled repulsive Fermi systems with 'nested' regions of the Fermi surface with finite density of fermionic states. The proposed theory of pairing via exchange with semiclassical fluctuations of finite amplitude populating the local minimum of potential energy of SDW/CDW inside the Q-balls differs from the standard Frohlich pairing mechanism via an exchange between fermions with incoherent bosons of infinitesimal amplitudes, e.g., phonons [16], spin–waves [3], or polarons [15,22]. The theory proposed here is simple enough, so that it could provide a basis for an analytically treatable calculations of spectral [23,24], transport, thermal [25], and electromagnetic [26] properties of the high temperature superconductors in pseudogap and superconducting states. As a first step, a theory of Q-balls formation is demonstrated in the above sections, which may naturally explain the linear dependence of T_c on superconducting density n_s in high-T_c superconducting compounds found experimentally [7]. It is also interesting to admit that obtained Q-ball solutions fall into the category of finite size thermodynamic time crystals, considered previously [27–30].

Funding: This research received no external funding.

Acknowledgments: The author acknowledges useful discussions with Serguey Brazovskii, Jan Zaanen, Carlo Beenakker, Konstantin Efetov and Andrey Chubukov. This research was supported by the Ministry of Science and Higher Education of the Russian Federation in the framework of Increase Competitiveness Program of NUST MISiS Grant No. K2-2020-038.

Conflicts of Interest: The author declares no conflict of interest.

References

1. Coleman, S.R. Q-Balls. *Nucl. Phys. B* **1985**, *262*, 263–283. [CrossRef]
2. Lee, T.D.; Pang, Y. Nontopological solitons. *Phys. Rept.* **1992**, *221*, 251–350. [CrossRef]
3. Abanov, A.; Chubukov, A.V.; Schmalian, J. Quantum-critical theory of the spin–fermion model and its application to cuprates: Normal state analysis. *Adv. Phys.* **2003**, *52*, 119–218. [CrossRef]
4. Scalapino, D.J. A common thread: The pairing interaction for unconventional superconductors. *Rev. Mod. Phys.* **2012**, *84*, 1383–1416. [CrossRef]
5. Ogata, M.; Fukuyama, H. The t-J model for the oxide high-T_c superconductors. *Rep. Prog. Phys.* **2008**, *71*, 036501. [CrossRef]
6. Spalek, J.; Zegrodnik, M.; Kaczmarczyk, J. Universal properties of high-temperature superconductors from real-space pairing: T-J-U model and its quantitative comparison with experiment. *Phys. Rev. B* **2017**, *95*, 024506. [CrossRef]
7. Uemura, Y.J. Universal correlations between T_c and n_s/m^* in high-T_c cuprate superconductors. *Phys. Rev. Lett.* **1989**, *62*, 2317–2320. [CrossRef] [PubMed]
8. Abrikosov, A.A.; Gor'kov, L.P.; Dzyaloshinski, I.E. *Methods of Quantum Field Theory in Statistical Physics*; Dover Publications: New York, NY, USA, 1963.
9. Derrick, G.H. Comments on nonlinear wave equations as models for elementary particles. *J. Math. Phys.* **1964**, *5*, 1252–1254. [CrossRef]
10. Mukhin, S.I. Negative Energy Antiferromagnetic Instantons Forming Cooper-Pairing Glue and Hidden Order in High-T_c Cuprates. *Condens. Matter* **2018**, *3*, 39. [CrossRef]
11. Schulz, H.J. Effective Action for Strongly Correlated Fermions from Functional Integrals. *Phys. Rev. Lett.* **1990**, *65*, 2462–2465. [CrossRef]
12. Tranquada, J.M.; Woo, H.; Perring, T.G.; Goka, H.; Gu, G.D.; Xu, G.; Fujita, M.; Yamada, K. Quantum magnetic excitations from stripes in copper oxide superconductors. *Nature* **2004**, *429*, 534–538. [CrossRef]
13. Tranquada, J.M. Neutron Scattering Studies of Antiferromagnetic Correlations in Cuprates. *arXiv* **2005**, arXiv:cond-mat/0512115.

14. Seibold, G.; Arpaia, R.; Peng, Y.Y.; Fumagalli, R.; Braicovich, L.; Di Castro, C.; Caprara, S. Strange metal behaviour from charge density fluctuations in cuprates. *Commun. Phys.* **2021**, *4*, 1–6.
15. Bianconi, A.; Missori, M. The instability of a 2D electron gas near the critical density for a Wigner polaron crystal giving the quantum state of cuprate superconductors. *Solid State Commun.* **1994**, *91*, 287–293. [CrossRef]
16. Eliashberg, G.M. Interactions between electrons and lattice vibrations in a superconductor. *JETP* **1960**, *11*, 696–702.
17. Witteker, E.T.; Watson, G.N. *A Course of Modern Analysis*; Cambridge University Press: Cambridge, UK, 1996.
18. Flügge S. *Practical Quantum Mechanics I*; Springer: Berlin/Heidelberg, Germany, 1971.
19. Chen, S.D.; Hashimoto, M.; He, Y.; Song, D.; Xu, K.J.; He, J.F.; Devereaux, T.P.; Eisaki, H.; Lu, D.H.; Zaanen, J.; et al. Incoherent strange metal sharply bounded by a critical doping in Bi2212. *Science* **2019**, *366*, 1099–1102. [CrossRef]
20. Bianconi, A.; Saini, N.L.; Agrestini, S.; Castro, D.D. The strain quantum critical point for superstripes in the phase diagram of all cuprate perovskites. *Int. J. Mod. Phys.* **2000**, *14*, 3342–3355. [CrossRef]
21. Li, H.; Zhou, X.; Parham, S.; Gordon, K.N.; Zhong, R.D.; Schneeloch, J.; Gu, G.D.; Huang, Y.; Berger, H.; Arnold, G.B.; et al. Four-legged starfish-shaped Cooper pairs with ultrashort antinodal length scales in cuprate superconductors. *arxiv* **2018**, arxiv:1809.02194v2.
22. Bianconi, A. On the Fermi liquid coupled with a generalized Wigner polaronic CDW giving high T_c superconductivity. *Solid State Commun.* **1994**, *91*, 1–5. [CrossRef]
23. Campi, G.; Bianconi, A.; Poccia, N.; Bianconi, G.; Barba, L.; Arrighetti, G.; Innocenti, D.; Karpinski, J.; Zhigadlo, N.D.; Kazakov, S.M.; et al. Inhomogeneity of charge-density-wave order and quenched disorder in a high-T_c superconductor. *Nature* **2015**, *525*, 359–362. [CrossRef]
24. Caprara, S. The ancient romans? route to charge density waves in cuprates. *Condens. Matter* **2019**, *4*, 60. [CrossRef]
25. Girod, C.; Leboeuf, D.; Demuer, A.; Seyfarth, G.; Imajo, S.; Kindo, K.; Kohama, Y.; Lizaire, M.; Legros, A.; Gourgout, A.; et al. Normal state specific heat in the cuprate superconductors $La_{2-x}Sr_xCuO_4$ and $Bi_{2+y}Sr_{2-x-y}La_xCuO_{6+\delta}$ near the critical point of the pseudogap phase. *Phys. Rev. B* **2021**, *103*, 214506. [CrossRef]
26. Li, L.; Wang, Y.; Komiya, S.; Ono, S.; Ando, Y.; Gu, G.D.; Ong, N.P. Diamagnetism and Cooper pairing above Tc in cuprates. *Phys. Rev. B* **2010**, *81*, 054510. [CrossRef]
27. Mukhin, S.I. Spontaneously broken Matsubara's time invariance in fermionic system: Macroscopic quantum ordered state of matter. *J. Supercond. Nov. Magn.* **2011**, *24*, 1165–1171. [CrossRef]
28. Mukhin, S.I. Euclidean action of fermi-system with "hidden order". *Phys. B Phys. Condens. Matter* **2015**, *460*, 264. [CrossRef]
29. Mukhin, S.I.; Galimzyanov, T.R. Classes of metastable thermodynamic quantum time crystals. *Phys. Rev. B* **2019**, *100*, 081103. [CrossRef]
30. Starkov, G.A.; Efetov, K.B. Phase transition into an instanton crystal state. *Phys. Rev. B* **2021**, *103*, 075121. [CrossRef]